DR. MIKIHIKO KAI (Orcid ID : 0000-0002-9113-6469)

Received Date : 19-Apr-2016

Revised Date : 28-Jan-2017

Accepted Date : 09-Feb-2017

Article type : Original Article

Predicting the spatio-temporal distributions of pelagic sharks in the western and central North Pacific

MIKIHIKO KAI[1], JAMES T. THORSON[2], KEVIN R. PINER[3], AND MARK N. MAUNDER[4,5]

[1]National Research Institute of Far Seas Fisheries (NRIFSF), Japan Fisheries Research and Education Agency
5-7-1, Orido, Shimizu, Shizuoka 424-8633, Japan
[2]Fisheries Resource Analysis and Monitoring Division, Northwest Fisheries Science Center, National Marine Fisheries Service (NMFS), NOAA
2725 Montlake Boulevard E, Seattle, WA 98112, USA.
[3]Southwest Fisheries Science Center, National Marine Fisheries Service (NMFS), NOAA
8901 La Jolla Shores Drive, La Jolla, CA 92037, USA.

[4]*Inter-American Tropical Tuna Commission*
8604 La Jolla Shores Drive, La Jolla, CA 92037-1508, USA.
[5]*Center for the Advancement of Population Assessment Methodology, Scripps Institution of Oceanography, La Jolla, CA 92093, United States*
*Correspondence to M Kai:
Tel: +81-543-36-6045
E-mail: kaim@affrc.go.jp

Running title: Spatiotemporal distribution of pelagic sharks

ABSTRACT

Spatio-temporal modeling estimates a species distribution function that represents variation in population density over space and time. Recent studies show that the approach may precisely identify spatial hotspots in species distribution, but have not addressed whether seasonal hotspots are identifiable using commonly available fishery data. In this study, we analysed the seasonal spatio-temporal distribution of pelagic sharks in the western and central North Pacific using fishery catch rates and a generalized linear mixed model with spatio-temporal effects. Different spatial distribution patterns were observed between two shark species. The hotspots of shortfin mako (SFM) appeared in the vicinity of the coastal and offshore waters of Japan and the Kuroshio-Oyashio transition zone (TZ), while the hotspots of blue shark (BSH) were widely distributed in the areas from the TZ to the waters of the Emperor Seamount Chain. SFM distribution changes seasonally with clear north-south movement, which follows higher sea surface temperatures (SST). However, preferred spring and summer water temperature was still colder than those in fall and winter, but not as cold as for BSH, which did not show seasonal north-south movement. BSH exhibits seasonal east-west movement apparently unrelated to temperature. The spatial fishing effort by season generally follows the seasonal movement of temperature possibly making SFM more vulnerable to the fishery than BSH. These findings could be used to reduce the capture risk of bycatch sharks and to better manage the spatial distribution of fishing for targeted sharks.

KEYWORDS: blue shark, hotspots, shortfin mako, spatio-temporal distribution, spatio-temporal model, template model builder

INTRODUCTION

Spatio-temporal patterns of areas of high fish density (also called hotspots) have been estimated using fishery-dependent data and distribution models (Su *et al*., 2011; Chang *et al*., 2012; Cambie *et al*., 2013; Cosandey-Godin *et al*., 2014; Yasuda *et al*., 2014; Ward *et al*., 2015; Thorson *et al*., 2016). Distribution models linked to environmental factors, in particular, sea surface temperature (SST), have demonstrated the importance of the role that the environment plays in determining spatial patterns (Felipe *et al*., 2011; Eriksen *et al*., 2012; Howell and Auster, 2012; Siders *et al*., 2013). A growing body of evidence exists that links shifts in distribution to temperature increases (e.g. climate change) (Perry *et al*., 2005; Kishi *et al*., 2009; Cheung *et al*., 2010; Kishi *et al*., 2010; Cheung *et al*., 2013; Ito *et al*., 2013; Yoon *et al*., 2015). Species temperature preferences have been attributed to higher survival and reproductive success (Lam *et al*., 2008).

Species distribution models estimate a distribution function which can be linked to environmental information to provide information on habitat. An understanding of the spatial distribution of a species and any potential environmental drivers can provide the scientific basis for habitat protection and fishery management that goes beyond simple catch limits (Chang *et al*., 2012; Ward *et al*., 2015). Extension of simple spatial models to include spatio-temporal modelling allows for estimation of the temporal variation in a population range and density. Spatial-temporal models can be used to estimate population abundance indices using formal statistical tools such as likelihood functions and sampling designs (Petitgas, 1998; Bez, 2002; Nishida and Chen, 2004; Roa-Ureta and Niklitschek, 2007; Kristensen *et al*., 2014; Petitgas *et al*., 2014; Thorson *et al*., 2015b, c). Recent studies (Shelton *et al*., 2014; Thorson *et al*., 2015b) show that the approach may yield more precise, biologically reasonable, and interpretable estimates of abundance than commonly used methods such as a generalized linear model (GLM; McCullagh and Nelder, 1989) and spatially stratified generalized linear mixed model (GLMMs; Stroup, 2012). In addition, spatial-temporal models may reduce bias associated with sample selection and fill in the spatial gaps associated with fishery-dependent data (Walter *et al*., 2014; Thorson *et al*., 2016).

Spatio-temporal considerations are especially important for pelagic sharks because they often exhibit spatial patterns in size and age (Nakano, 1994; Nakano and Seki, 2003). These patterns arise from differences in the spatial distribution of different cohorts, perhaps arising from the biological partitioning of available habitat. Such segregation is thought to reduce intraspecific cannibalism and competition (Nakano, 1994). Shortfin mako (SFM) (*Isurus oxyrinchus*) and blue shark (BSH) (*Prionace glauca*) are widely caught in the North Pacific (Hiraoka *et al*., 2016; Ohshimo *et al*., 2016). Juveniles and subadults of these species (mainly 60-240 cm pre-caudal length

(PCL)/0-20 years old for SFM and 60-160 cm PCL/0-6 years old for BSH) are primarily caught by Japanese commercial shallow-set longliners in the western and central North Pacific. The spatial distributions of these commercial fisheries change seasonally corresponding to the seasonal movement of the target species, primarily swordfish (*Xiphias gladius*) (Ishimura and Bailey, 2013; Hiraoka *et al*., 2016). Although BSH is occasionally also targeted, SFM is exclusively a non-target bycatch species. In the North Pacific, the standardized catch rates of BSH are higher than those of SFM (Clarke *et al*., 2013), indicating that either the population size of BSH is larger than that of SFM or the SFM is less likely to be caught in commercial fishing gear. The commercial fishery data covers a wide range of areas (21-45°N and 135°E-180°) and seasons, providing enough information to estimate seasonal changes in the species distribution function for juveniles and sub-adults of SFM and BSH in the western and central North Pacific.

Previous studies (Hiraoka *et al*., 2016; Ohshimo *et al*., 2016) have attempted to standardize CPUE of BSH and SFM using the commercial fisheries data. Hiraoka *et al*. (2016) and Ohshimo *et al*. (2016) used standard methods such as GLM or generalized additive model (GAM; Wood, 2006). Recent developments in spatio-temporal modelling, such as those proposed by Thorson *et al*. (2015b), may provide an improvement over conventional time-series and spatially stratified models because it estimates the density in unsampled areas by imputation (Carruthers *et al*., 2011). Accounting for unsampled stations or providing more information to poorly sampled areas may help reduce biases caused by the spatial and temporal heterogeneity of both fish and fishery. Spatio-temporal modelling may also improve the proportionality between CPUE and true population abundance by allowing for proper areas weighting of the index rather than data weighing or ad hoc area weighing that are common in typical GLM CPUE analyses.

In this study, we sought to answer the following questions: (1) what is the spatial distribution of SFM and BSH, and does it vary predictably among seasons?; (2) is the spatial distribution associated with seasonal changes in SST? (does temperature explain seasonal variation in distribution, or is there a substantial component of seasonal distribution shift that is unexplained by temperature?); and (3) are seasonal patterns stable enough to recommend spatial management that changes among seasons to protect bycatch shark species? We addressed these questions by applying a spatio-temporal regression approach using a generalized linear mixed model to generate spatial maps of the distribution of catch rates and to fill in spatial gaps of the fishery-dependent catch rate. We then identified potential hotspots of the pelagic sharks in the western and central North Pacific Ocean and compared the spatio-temporal distributions of targeted and non-targeted sharks with SST.

MATERIALS AND METHODS

Data sources

The available data covered wide areas of the western and central North Pacific (Fig. 1). The SST in these areas ranged between 0°C and 30°C (see https://podaac.jpl.nasa.gov /dataset/NCDC-L4LRblend-GLOB-AVHRR_OI, accessed 28 Jan. 2017). The original SST data has a resolution of 0.25 × 0.25 degree square per day. The data were averaged by year and three-month quarters with a resolution of 1 × 1 degree square. The region of the western and central North Pacific was broadly defined as the Oyashio (cold water) Current, the Kuroshio (warm water) Current, the Kuroshio-Oyashio transition zone (TZ) and Mixed water regions (Fig. 1), which is one of the main oceanic features of the North Pacific (Roden, 1991; Yasuda *et al*., 1996, 2000; Yoshinari *et al*., 2001; Inoue *et al*., 2003; Yasuda, 2003). The Kuroshio and Oyashio currents meet in the Pacific east of Japan and a complex oceanic feature associated with warm and cold fronts and eddies of various scale appears in the TZ and Mixed water region (e.g., Reid, 1965; Kawai, 1972; Hasunuma, 1978). The western North Pacific therefore provides an important habitat for many species of epipelagic nektonic fishes and squids that are highly migratory between subtropical and subarctic areas (Pearcy, 1991). The Emperor Seamount Chain is located in the central North Pacific (30–55°N and approximately 170°E), representing another oceanic feature that has a high potential for biological resources due to the interaction of ocean currents and complex topography (Boehlert, 1986, 1988). Four seasons (quarters (Q) 1 to 4) were defined as follows: Q1 was spring from Jan. to Mar.; Q2 was summer from Apr. to Jun.; Q3 was fall from Jul. to Sep.; and Q4 was winter from Oct. to Dec..

We analyzed catch and effort data of Japanese shallow-set longliners operating in the North Pacific (north of the equator) from 2010 to 2014 to estimate the seasonal distribution of pelagic sharks in recent years. Data from these years can provide the estimates of spatio-temporal distribution for the species. The set-by-set data used in this study included information on species of sharks, catch number, amount of effort (number of hooks), number of branch lines between floats (hooks between floats: HBF) as a proxy for gear configuration, and location (latitude and longitude) of set, with a resolution of 1 × 1 degree square. Only the shallow-set data were used in the analysis. The shallow-set data is used because fishermen change the depth of the gear to change the target species, and is identified by the number of HBF, which determines the fishing depth (Nakano *et al*., 1997). We defined the shallow-set fishery by the use of a small number of HBF (3-5 hooks). The hooks of the regular longline gear are estimated to hang at the depth around 50 to 120 m (Suzuki *et al*., 1977).

Spatio-temporal model

We developed a model that accounts for both seasonal and interannual variability in the distribution of shark species in the Pacific Ocean, while accounting for differences in sampling intensity between locations, seasons and years. We also included linear and quadratic terms for SST as spatial covariates which were assumed to impact density. We used a hierarchical spatio-temporal model for this task, so that we could explicitly decompose variance into components representing among-year and within-year variation. We then used the model to predict density at unsampled locations and times, to provide a best-estimate of the distribution of species. Spatio-temporal modelling of CPUE data assumes that species density at nearby locations should have similar density estimates during each time interval. The correlation between statistical stations (latitude and longitude) in a given time interval (governed by fixed effects that are estimated from the data) was then used to estimate catch rates in a period (year and quarter) for all stations, including stations that do not have data in a given period. We then compared these predictions with temperature data for each species, to evaluate whether each species has temperature preferences and also what regions of the Pacific each species prefers during each season. Although previous analyses have used fishery-dependent catch rate data for species distribution modelling (e.g., Thorson *et al*., 2016), this study is the first in our knowledge to model both within- and among-year (i.e., seasonal and interannual) shifts in distribution using spatio-temporal models for fishery dependent data.

Model description

The spatio-temporal model estimated the density $d\,(s, t, q)$ in each station s (latitude and longitude with a resolution of 1×1 degree square), year-quarter t (signifying a three-month quarter, where $t = 1$ in signifies Q1 2010 and $t = 20$ signifies Q4 2014), and quarter q (signifying a three-month quarter, where $q = 1$ in signifies Q1 and $q = 4$ in signifies Q4). We modelled the temporal variation at the scale of 3-month intervals, given that both species showed strong variable distributions among seasons and years. Each station, year-quarter, and quarter had the density:

$$d(s,t,q) = \exp\left(d_0(t,q) + \gamma(s) + \theta(s,t) + \omega(s,q) + \sum_{j=1}^{n_j} \beta_j x_j(s,t)\right), \quad (1)$$

where $d_0(t,q)$ represents temporal variation (the intercept for each year-quarter t and quarter q), $\gamma(s)$ represents spatial variation (the average density in station s relative to the average station), $\theta(s,t)$ and $\omega(s,q)$ represents spatio-temporal variation (additional variation in density for station s and year-quarter t, and for station s and quarter q, respectively, after accounting for purely spatial and temporal variation), and β_j represents the impact of covariate j with value $x_j(s,t)$ on density for station s and year-quarter t. Spatial variation $\gamma(s)$ is modeled as a

Gaussian random field (GRF), which reduces to a multivariate normal distribution (MVN) when evaluated at a finite set of stations (Thorson *et al.*, 2015c):

$$\boldsymbol{\gamma} \sim MVN(\mathbf{0}, \sigma_\gamma^2 \cdot \mathbf{R}_{\boldsymbol{spatial}}), \tag{2}$$

where σ_γ is the marginal standard deviation (SD) of spatial variation $\boldsymbol{\gamma}$ and $\mathbf{R}_{\boldsymbol{spatial}}$ is spatial correlation for the random field:

$$\mathbf{R}_{\boldsymbol{spatial}}(s, s') = \text{Matérn}\left(\frac{|(s-s')|}{\kappa}\right), \tag{3}$$

where *s* and *s*' are the location of 2 spatial stations, κ defines the rate at which correlations drop with increasing distance, and Matérn (|(*s*-*s*')|) is the Matérn correlation function, which calculates the correlation between $\boldsymbol{\gamma}$ at stations *s* and *s*' given their distance |*s*-*s*'|. We used the Matérn correlation function because previous research demonstrated how the probability of GRFs could be calculated efficiently given this assumption (Diggle and Ribeiro, 2007; Roa-Ureta and Niklitschek, 2007; Lindgren *et al.*, 2011). GRF is a convenient statistical approach for implementing a 2-dimentional smoother for a response variable (in this case, catch) over spatial dimensions (Thorson *et al.*, 2015b). The spatial-temporal variation, $\theta(s,t)$, was modeled by combining the GRF for spatial variation with first-order autoregressive process for temporal variation at each site:

$$\text{vec}(\boldsymbol{\theta}) \sim MVN(\mathbf{0}, \sigma_\theta^2 \cdot \mathbf{R}_{\boldsymbol{spatial}} \otimes \mathbf{R}_{\boldsymbol{AR1}}), \tag{4}$$

where $\text{vec}(\boldsymbol{\theta})$ is the vectorized value of matrix $\boldsymbol{\theta}$, σ_θ is the marginal SD of spatio-temporal variation $\boldsymbol{\theta}$**,** $\otimes$ is the Kronecker product where if **A** is an *m* x *n* matrix and **B** is a *p* x *q* matrix, then the Kronecker product $\mathbf{A} \otimes \mathbf{B}$ is the *mp* x *nq* block matrix:

$$\mathbf{A} \otimes \mathbf{B} = \begin{bmatrix} \boldsymbol{a_{11}}\mathbf{B} & \cdots & \boldsymbol{a_{1n}}\mathbf{B} \\ \vdots & \ddots & \vdots \\ \boldsymbol{a_{m1}}\mathbf{B} & \cdots & \boldsymbol{a_{mn}}\mathbf{B} \end{bmatrix}, \tag{5}$$

and $\mathbf{R}_{\boldsymbol{AR1}}$ is the temporal component of variance in spatio-temporal variation $\boldsymbol{\theta}$**:**

$$\mathbf{R}_{AR1}(t, t') = \rho^{|t-t'|}, \tag{6}$$

where ρ is a parameter governing autocorrelation and |*t*-*t*'| is the difference in time among samples in year-quarter *t*. The other spatial-temporal variation, $\omega(s,q)$ was modeled by the same methods as $\theta(s,t)$. In the following, we included a quadratic effect of sea surface temperate, SST (i.e., $n_j = 2$ where $x_1(s,t)$ is average SST and $x_2(s,t)$ is SST-squared for that station and year-quarter). We estimated a separate SD for spatial (σ_γ) and spatio-temporal (σ_θ, and σ_ω) components, but estimated the same decorrelation distance (κ) for the processes, using the implicit assumption that dynamics were defined by a "characteristic scale" that defined decorrelation distance for both. Following the parameterization from Lindgren *et al*. (2011), we estimated a magnitude parameter η for each spatial and spatio-temporal process, and the corresponding marginal SD was then calculated as:

$$\sigma_{\gamma} = 1/\sqrt{4\pi\eta_{\gamma}^{2}}, \tag{7}$$

where other marginal SDs (i.e., σ_{θ}, and σ_{ω}) were calculated similarly (from η_{θ}, and η_{ω}).

Expected catch c_i^* is a function of density and fishing effort f_i (number of hooks), $c_i^* = d(s_i, t_i, q_i) f_i$, and was then compared with the observed catch (in numbers) c_i for the *i*-th observation, in station s_i , year-quarter t_i, and quarter q_i. Count data of the sharks typically include many observations with zero catch and a few observations with large values when the sharks were aggregated (Bigelow *et al*., 1999; Ward and Myers, 2005). We used a negative-binomial distribution:

$$c_i \sim NegBin(c_i^*,\ c_i^*(1+\sigma_1) + {c_i^*}^2\sigma_2), \tag{8}$$

where *NegBin* (*x*,*y*) is a negative binomial distribution with mean *x* and variance *y* (Lindén and Mäntyniemi, 2011). We used this mean-variance parameterization (rather than more-common versions) so that we can estimate two parameters (rather than just one) to govern the mean-variance relationship. Parameters representing temporal variation (d_0), spatial covariance (κ and η_{γ}), spatial-temporal covariance (η_{θ}, η_{ω}, ρ_{θ}, and ρ_{ω}), density covariate (β_1 and β_2) and residual variation (σ_1 and σ_2) were estimated as fixed effects while integrating across random effects representing spatial (station) and spatio-temporal (station and year-quarter, and station and quarter) variations (see Supporting information). This integral was approximated using the Laplace approximation, and the fixed effects were estimated using gradient information as provided by Template Model Builder (TMB; Kristensen, 2015), which is an R package (R Core Team, 2013) for fitting statistical latent variable models to data. It was inspired by ADMB (Fournier *et al*., 2012). The details of TMB are described on the website (see http://www.admb-project.org/developers/tmb/, accessed 28 Jan. 2017). Further details regarding GRF estimation can be found in Thorson *et al*. (2015b, c).

After estimating the fixed effects (year and quarter, effect of SST, and parameters for the random effects) by maximizing the marginal likelihood of the data, the distributions for SFM and BSH were predicted from the fixed and random effects. Average quarterly and year-quarter specific spatial distributions of standardized CPUEs for both species were compared with those of effort. When visualizing distribution maps in each quarter, we also overlapped the isoclines of the mean observed SST to examine the relationship between those distributions and seasonal and annual changes of the mean observed SST. In the following, we presented and interpreted maps of density that include the effect of fixed effects (e.g., temperature) and random effects (e.g., residual spatial variation). We defined "preferred habitat" as the locations where the predicted catch rate was greater than the mean value of each shark. Here, the average catch rate for each quarter was calculated as:

$$\bar{d}(s,q) = \frac{1}{5}\sum_{t=1}^{5}\sum_{q'=1}^{4} I(q = q')d(s,t,q), \tag{9}$$

where $d(s,t,q)$ is defined in Eq. (1), $\bar{d}(s,q)$ is the average density at location s for quarter q averaged over the five instances of that quarter within the 20 modeled intervals, and $I(q = q')$ is an indicator function that equals one if the quarter q associated with time-period t is Q and zero otherwise, and where we plotted the density relative to its average for a given quarter:

$$d^{*}(s,q) = \frac{\bar{d}(s,q)}{\left(\frac{1}{n_s}\sum \bar{d}(s,q)\right)}. \tag{10}$$

Model convergence was confirmed using the hessian matrix (confirming that the hessian is positive definite) and by ensuring that the maximum absolute value of the final gradient of parameters was less than 0.0001. The changes in predicted catch rates were compared among multiple models (Table 1). We used Akaike Information Criterion (AIC; Akaike, 1973) to identify which model had greater support given available data: this model-selection is appropriate given that TMB implements maximum marginal likelihood estimation. We also interpreted the importance of including or excluding temperature by recording how much the inclusion of temperature decreases the marginal SD of spatial or spatio-temporal variation.

RESULTS

The most complicated model (M-12) included purely spatial variation (variation in log-expected density among stations that was constant over time), spatio-temporal variation among seasons (variation in log-expected density that varied by quarter), and spatio-temporal variation among all periods (variation in log-expected density for every combination of quarter and year). AIC identified this saturated model as the most parsimonious model (Table 1) and the maximum gradient was less than 0.0001 (the 4.73E-08 for BSH, 1.38E-05 for SFM). Including the seasonal component for spatio-temporal variation substantially decreased the marginal SD of spatial and spatio-temporal variation among all periods (e.g., compare the M-5 (or M-11) with M-6 (or M-12) for two species). We therefore used the saturated model (M-12) to predict the spatio-temporal maps and to elucidate the seasonal changes of their preference temperature.

Seasonal changes of the spatial distribution of SFM showed that there was a strong relationship between the predicted catch rate and SST that resulted in the seasonal pattern of north-south movement (left panels in Fig. 2, also see the supplementary material). The locations of hotspots were coastal and offshore waters of Japan, and those catch rates were high (catch rate 2–5 times the average) in the water of 15–25°C throughout all seasons (left panels in Fig. 2). For Q1, the predicted catch rates were high (catch rate = 2–3 times the average) in wide ranges of southern waters (approximately 30–35°N and 140°E –180°). For Q2, the predicted catch rates were high (catch rate = 2–4 times the average) in the coastal waters of Japan, and hotspots appeared along with the Kuroshio-Oyashio TZ (33-37°N and 140–150°E). For Q3, high catch rates (catch rate = 3–5 times the average) were observed in the coastal waters of Japan (33–40°N and 140–145°E). For Q4, the hotspots (catch rate = 2–3 times the average) appeared in the offshore areas with an expansion to the southern and eastern waters (30–40°N and 140–170°E). The seasonal pattern of north-south movement was consistent over the years in our study (Fig. 3).

Unlike SFM, BSH did not show a strong relationship between the predicted catch rate and SST (mid panels in Fig. 2, also see the supplementary material). In contrast, BSH showed seasonal east-west movement with a more westward distribution in Q1 and Q2. However, the east-west movement was less consistent over the years in our study (Fig. 4). The predicted catch rates throughout all seasons were high (catch rate = 2–4 times the average) in the northern waters, where the SST was 10–25°C (mid panels in Fig. 2). However, the locations of hotspots varied throughout the western and central North Pacific. For Q1, the predicted catch rates were high (catch rate = 2–3 times the average) in the offshore waters along with the Kuroshio-Oyashio TZ and Mixed water region (30–37°N and 145–163°E) and around the water of Emperor Seamount Chain (35–42°N and 168°E–180°). For Q2, hotspots (catch rate = 2–4 times the average) were observed in nearly the same areas as those in Q1. For Q3, hotspots (catch rate = 2–4 times the average) were mainly observed around the water of The Emperor Seamount Chain (35–40°N and 168°E –180°). For Q4, hotspots (catch rate = 2–4 times the average) were observed in the offshore waters along with the Kuroshio extension (35–38°N and 148–163°E) and water of The Emperor Seamount Chain (35–40°N and 168°E–180°). The areas of high fishing effort were not necessarily the same as areas of high catch rates for both species throughout all seasons (right panels in Fig. 2).

The predicted catch rates (relative value to mean value) against SST showed that the SST associated with high catch rates (more than 1) varied by season and by species (Fig. 5). The high catch rates of SFM were observed in the water where the SST was between 9.9°C and 27.0°C throughout all seasons, while the high catch rates of BSH were observed in the water where the SST was between 6.3°C and 26.5°C (Table 2, Fig. 5). The high catch rates of SFM in Q1, Q2, Q3, and Q4 were observed in the water where the SST was 9.9–21.8°C, 10.0–21.5°C, 14.9 –27.0°C, and 10.4 –23.8°C, respectively (Table 2). The high catch rates of BSH in Q1, Q2, Q3, and Q4 were observed in the water where the SST was 6.3–19.1°C, 6.5–20.4°C, 14.9–26.5°C, and 9.4–23.2°C, respectively (Table 2). These findings indicated that high catch rates of both sharks appeared in similar wide ranges of SST;

however, the seasonal density plots in Fig. 5 and Table 2 showed that SFM stayed in the warmer water in comparison with the BSH (i.e. the ranges of SST for SFM was 17.5–21.5°C from the 25–75% quantile and those for BSH was 13.9–19.8°C). The seasonal density plots also showed that those were negatively skewed for all plots of both sharks especially for SFM (Fig. 5). These findings suggested that SFM and BSH preferred to stay in the relatively warmer water in each season, and SFM preferred warmer water than BSH.

SFM were distributed in the southern water around 30–37°N in Q1 and Q2 when the water temperature was cooler in the northern water around 40°N (left panels in Fig. 2 and Fig. 3). However, the water temperature experienced by SFM was still cooler in Q1 and Q2 than in the other half of the year (Table 2 and Fig. 5). By contrast, BSH stayed in the north throughout the year (mid panels in Fig. 2 and Fig. 4) and therefore experienced much lower temperatures than SFM during Q1 and Q2 (Table 2 and Fig. 5).

Comparing the predicted density of both species against SST also showed that SFM preferred warmer water than BSH (see Supporting information).

DISCUSSION

A clear relationship between the seasonal distribution of the two shark species and SST exists, but the relationship differed between the two species. SFM preferred the temperate waters of approximately 15–25°C, making latitudinal movements matching seasonal changes in SST. A similar preferred range in temperatures was documented by Kai *et al.* (2015) for juvenile SFM caught by Japanese driftnet and longline fisheries. Casey and Kohler (1992) documented narrower range of 17–22°C, based on a large tagging study in the western North Atlantic. Within the preferred temperature, our results showed SFM to be distributed evenly in both coastal and offshore areas in the western North Pacific. This region is characterized by high productivity, due to the thermal fronts of the Kuroshio-Oyashio transition zone (Pearcy, 1991; Yasuda *et al.*, 1996; Yasuda *et al.*, 2000; Yasuda, 2003). Fronts where warm water and cold water mix, may cause prey to aggregate at continental shelves, concentrating predators (Young *et al.*, 2001).

BSH were also found in association with SST. In contrast to SFM, BSH were found in association with colder water and showed seasonal changes in their spatial distribution in a longitudinal direction. Ohshimo *et al.* (2016) reported that the SST at with elevated catch of BSH was colder than those for SFM, and their results were similar to ours. Our study relied on data from a large-scale fishery, but more direct tagging observations of depth and temperatures occupied by pelagic sharks has been studied at smaller scales. Musyl *et al.* (2011) investigated the movement patterns using pop-up satellite archival tags (PSATs) and showed that BSH and SFM in the Pacific

Ocean experienced a wide range of temperatures (95% of temperatures occupied were from 9.7–26.9°C and 9.4–25.0°C, respectively). Queiroz *et al*. (2010) recorded the movements of BSH in the northeastern Atlantic Ocean using satellite-linked archival transmitters and showed that vertical movements ranged from the surface to a maximum depth of 696 m, and water temperatures varied from 10.6°C to 24.6°C. BSH also demonstrated a wide vertical distribution, inhabiting depths from the surface to a maximum of 1160 m and spanning water temperatures from 7.2°C to 27.2°C (Queiroz *et al*., 2012). Stevens (2010) studied the movements and behaviour of ten BSH off eastern Australia and showed that BSH were mainly in 17.5–20.0°C. These results supported the temperature ranges of SFM and BSH in our study (Table 2).

The spatial fishing effort was distributed in the range of SST (15–25°C) where the mean SST across the water was lower in Q1 and higher in Q3 (right panels in Fig. 2). The exception of the spatial distribution of fishing effort in the southern water in Q2 was caused by Japanese shallow-set longliner mainly targeting swordfish in this area (Hiraoka *et al*., 2016). The spatial distribution of BSH, which is one of the target species, is supposed to follow the distribution of the fishing effort, however, this was not observed in Q1 and Q2 (mid and right panels in Fig. 2). By contrast, the spatial distribution of the predicted CPUEs for SFM followed the spatial distribution of the fishing effort (left and right panels in Fig. 2). SFM was therefore more sensitive to the changes in the SST than BSH that resulted in the clear seasonal north-south movement. Our results suggested that latitudinal shifts in fishing effort and SFM nominal CPUE coincided, but there was no clear relationship between high nominal CPUE and high fishing effort longitudinally (see Supporting information). This was because the spatio-temporal modeling approach can reduce the biases of the spatio-temporal distribution of catch rate through the standardization of the nominal CPUE. Understanding of fishery data is complex (Thorson *et al*., 2016), which emphasizes the need for properly accounting for potential biases before drawing conclusions.

The spatio-temporal modeling approach differs from the more commonly used methods of analyzing fishery CPUE data (Design-based, GLM, GLMM) by explicitly considering the spatial and temporal correlation of the data (Petitgas, 2001; Shelton *et al*., 2014; Thorson *et al*., 2015b). A primary concern is the spatial correlation associated with regions of high or low abundance. Perhaps the greatest advantage of the spatio-temporal modeling approach is the ability to estimate density in unsampled regions by imputation (Carruthers *et al*., 2011). However, as Thorson *et al*. (2015b) noted, this method may result in biased estimates when fishing effort is correlated with population abundance (Diggle *et al*., 2010). For bycatch species, such as SFM, this may not be a problem, while BSH may be a problem because BSH is occasionally one of the target species of the Japanese shallow-set longliners, as previously described. Therefore, the spatio-temporal modeling approach may over-weight data in areas with a large amount of data (i.e., areas with targeted fishing) relative to a model that explicitly accounts for preferential sampling. However, commercial catch and effort data are currently the only source of information to map spatio-temporal distribution of pelagic sharks in the western and central North Pacific. In addition, the spatio-temporal modeling approach is a better way to reduce the bias and variance caused by the fisheries targeting areas of high abundance than a nonspatial modeling approach. In future work, large tagging studies in the western and central North Pacific will be necessary to verify the accuracy of the estimation of the spatio-temporal modeling approach.

Generalized linear mixed modeling commonly bases the AIC on the marginal likelihood with the random effects integrated out, which may lead model selection to choose models including more covariates than is optimal (Greven and Kneib, 2010). Hoeting *et al*. (2006) demonstrated that the corrected AIC for a spatio-temporal model was superior to the standard approach of ignoring spatial correlation in the selection of explanatory variables. However, we used a standard AIC because the corrected AIC is similar to the standard AIC for large sample sizes.

The environmental changes such as an SST can have a large influence on catchability (Stoner, 2004; Maunder *et al*., 2006). Several past studies took the impact of environmental variables on the CPUE of blue sharks into account (Bigelow *et al*., 1999; Walsh and Kleiber, 2001; Carvalho *et al*., 2011; Mitchell *et al*., 2014). However, the choice of explanatory variables in developing fishery oceanographic relationships depends on the objectives of the analysis and the spatiotemporal scales of available environmental data, e.g., time-series measurements or long-term (climatological) averages (Bigelow *et al*., 1999). Our study used environmental data (i.e. SST) for 1 x 1 spatial and year-quarter temporal scales to clarify the spatial distribution associated with seasonal changes in SST.

The method proposed here can identify hotspots of pelagic sharks, and this information is useful not only for the management of target species but also to reduce the capture risk of bycatch species (Cosandey-Godin *et al*., 2014; Ward *et al*., 2015). Time and area closures are one of the effective methods to mitigate the impacts of bycatch (Dunn *et al*., 2011; Cambie *et al*., 2013), and is particularly effective at protecting vulnerable life history stages without overly constraining a directed fishery.

The marginal SD of spatial random variation of the best model (M-12) went to zero for the SFM and dropped in half for BSH in comparisons with the model without the station and quarter random effect (M-11) (Table 1). These findings suggested that the station and quarter random effect had a profound implication, particularly for SFM. The seasonal north-south movement of SFM to maintain a constant range of SST may have a large impact on the results. When SST terms were included in the models (compare the models M-5 and M-6 with models M-11 and

M-12 respectively) for both species, the marginal SDs of all random variations dropped for both species, but more for BSH (Table 1). These findings suggested that spatial-temporal variations for BSH were more influenced by SST than those for SFM. The seasonal east-west movement of BSH, which is apparently unrelated to SST, may have a large impact on the results because the mean SST at the high predicted catch rates was more different among seasons for BSH than for SFM (Table 2).

In this study, we didn't focus on the annual changes in the abundance index. Calculating the annual abundance index requires choosing whether the abundance index is calculated based on the average over all quarters or is derived from a specific quarter. If the seasonal changes in the spatial distribution are not fundamentally environmentally driven, then it might be reasonable to choose a season when all the fish are in the area to calculate the index. The seasonal changes in the predicted CPUEs for SFM were more stable than those for BSH, exemplified by a remarkable peak in predicted CPUE observed in Q 2 for BSH (see Supporting information). It may be that BSH shifted their spatial distribution to northern areas above 40°N in other seasons resulting in higher predicted CPUE in Q2 than in other seasons. Based on these arguments researchers attempting to produce a standardized abundance index of SFM should consider using only a single quarter and for BSH an average over all quarters.

Spatial and temporal changes in the sex, size and age structure of the population is an important factor in abundance indexes because blue sharks show evidence of size (Nakano and Nagasawa, 1996) and sex segregation (ratio of BSH, male:female, 1.00 : 0.34) (Mucientes *et al*., 2009). Several previous studies (Kristensen *et al*., 2014; Nielsen *et al*., 2014; Thorson *et al*., 2015a; Jansen *et al*., 2016; Kai *et al*., 2017) developed the spatio-temporal dynamics modeling incorporating the size-structured populations. In this study, however, we did not explicitly account for the age or length in the estimated species distribution function. Inclusion of the sex and length data into the model might permit future analyses to estimate size and sex-specific distributions, and we recommend this line of future research to potentially account for the impact of changes in sex- and length-structure on the distribution for each species. Additionally, sex- , age and size-specific relative abundance might provide useful information to understand the life history and stock condition, such as pupping ground, feeding ground and strength of the recruitment. Moreover, it is possible to show the yearly changes of sex and age-specific spatio-temporal maps, as well as annual trends of the standardized catch rate by sex and age classes. These maps might provide the geographical segregation of species by sex, age and size classes from year to year, and the trends of age-0 class relative abundance might provide the yearly changes of recruitment fluctuation.

An alternative explanation for the seasonal pattern in spatial distribution is the segregation of size classes. A schematic BSH migration model suggested by Nakano (1994) demonstrated that the nursery area was located in the northern areas, and adults mainly occurred in equatorial water to the south of the nursery area. Additionally, it is reasonable that the parturition and nursery grounds are located in the subarctic boundary, where there is a large prey biomass for young shark. In particular, the surroundings of The Emperor Seamount Chain and other complex topography may be the sites of aggregations of many highly migratory species, such as tunas, sharks and marine mammals that feed on prey aggregations due to high productivity (Boehlert, 1986, 1988). If the migration of the BSH and SFM in the north Pacific is not determined by physical environmental information such as an SST, but by yearly migration route programmed a priori and navigated astronomically, the results could be only a pseudo-correlation. We could answer this kind of questions by comparing the year-quarter specific change of the migration root by using the PSATs in future work. Shifts in fishermen behaviors targeting bycatch species in some seasons are possibilities. Aires-da-Silva *et al*. (2008) documented shifting fishing effort toward pelagic sharks occurring during times of low swordfish abundance in Azorean waters. A similar behaviour has been hypothesized for some Japanese longliners when the catch rate of swordfish is low.

In conclusion, SFM and BSH changed their spatial distribution by season, possibly in accordance with changes in the SST, but two species showed different spatial distribution patterns. The hotspots of shortfin mako (SFM) appeared in the vicinity of the coastal and offshore waters of Japan along with Kuroshio-Oyashio transition zone (TZ), while the hotspots of blue shark (BSH) were widely distributed in the areas from the TZ to the water of The Emperor Seamount Chain. SFM fundamentally changed their seasonal distribution latitudinal direction between north and south and maintained higher SST than BSH, while BSH fundamentally changed their seasonal distribution longitudinally between east and west in the northern water which apparently unrelated to SST and maintained lower SST than SFM. SFM plainly prefer to stay in slightly higher SST around 18–22°C, while BSH prefer to stay in slightly lower SST around 14–20°C. The spatial fishing effort by season generally follows the seasonal movement of temperature possibly making SFM more vulnerable to the fishery than BSH. These findings could be used to reduce the capture risk of bycatch sharks and to better manage the spatial distribution of fishing for targeted sharks.

ACKNOWLEDGEMENTS

The authors sincerely wish to thank editor and four anonymous reviewers and all members of the ISC shark Working Group that made invaluable comments and suggestions. We also thank Kasper Kristensen and the many contributors to the Template Model Builder software. Finally, we are grateful to Bill Bayliff for carefully proofreading manuscript. This work was supported in part by a grant-in-aid from the Japan Fisheries Agency.

REFERENCES

Aires-da-Silva, A., Ferreira, R. L. and Pereira, J. G. (2008) Case study: Blue Shark Catch-Rate Patterns from the Portuguese Swordfish Longline Fishery in the Azores. In: Sharks of the Open Ocean: Biology, Fisheries and Conservation. M. D. Chami, E. K. Pikitch and E. A. Babcock (ed.) Oxford: Blackwell Publishing, pp. 230–235.

Akaike, H. (1973) Information theory as an extension of the maximum likelihood principle. In: 2nd International Symposium on Information Theory. B. N. Petrov and F. Csaki (ed.) Budapest: Akademiai Kiado, pp. 267–281.

Bez, N. (2002) Global fish abundance estimation from regular sampling: the geostatistical transitive method. *Can. J. Fish Aquat. Sci.* **59:**1921–1931.

Bigelow, K. A., Boggs, C. H. and He, X. (1999) Environmental effects on swordfish and blue shark catch rates in the US North Pacific longline fishery. *Fish Oceanogr.* **8:**178–198.

Boehlert, G. W. (1986) Productivity and population maintenance of seamount resources and future research directions. Biology of the transition region. *NOAA Tech. Rep. NMFS* **43:**95–101.

Boehlert, G. W. (1988) Current–Topography Interactions at Mid-Ocean Seamounts and the Impacts on Pelagic Ecosystems. *GeoJournal* **16:**45–52.

Cambie, G., Sanchez, C. N., Mingozzi, T., Muiño, R. and Freire, J. (2013) Identifying and mapping local bycatch hotspots of loggerhead sea turtles using a GIS-based method: implications for conservation. *Mar. Biol.* **160:**653−665.

Carruthers, T. R., Ahrens, R. N., McAllister, M. K. and Walters, C. J. (2011) Integrating imputation and standardization of catch rate data in the calculation of relative abundance indices. *Fish. Res.* **109:**157–167.

Carvalho, F. C., Murie, D. J., Hazin, F. H. V., Hazin, H. G., Leite-Mourato, B. and Burgess, G. H. (2011). Spatial predictions of blue shark (*Prionace glauca*) catch rate and catch probability of juveniles in the south-west Atlantic. *ICES J. Mar. Sci.* **68:**890–900. doi:10.1093/icesjms/fsr047

Casey, J. G. and Kohler, N. E. (1992) Tagging studies on the shortfin Mako Shark (*Isurus oxyrinchus*) in the western North Atlantic. *Mar. Freshwater Res.* **43:**45–60.

Chang, Y. J., Sun, C. L., Chen, Y., Yeh, S. Z. and Dinardo, G. (2012) Habitat suitability snalysis and identification of potential fishing grounds for swordfish, *Xiphias gladius*, in the South Atlantic Ocean. *Int. J. Remote Sens.* **33:**7523 −7541.

Cheung, W. W. L., Lam, V. W. Y., Sarmiento, J. L., Kearney, K., Watson, R., Zeller, D. and Pauly. D. (2010) Large-scale redistribution of maximum fisheries catch potential in the global ocean under climate change. *Glob. Change Biol.* **16:**24–35.

Cheung, W. W. L., Watson, R. and Pauly, D. (2013) Signature of ocean warming in global fisheries catch. *Nature* **497:**365 −368.

Clarke, S. C., Harley, S. J., Hoyle, S. D. and Rice, J. S. (2013) Population trends in Pacific Oceanic sharks and the utility of regulations on shark finning. *Conserv. Biol.* **27:**197−209.

Cosandey-Godin, A., Krainski, E. T., Worm, B. and Flemming, J. M. (2014) Applying Bayesian spatiotemporal models to fisheries bycatch in the Canadian Arctic. *Can. J. Fish. Aquat. Sci.* **72:**186–197.

Diggle, P. J. and Ribeiro, P. (2007) Model-Based Geostatics. Springer, New York, 228 pp.

Diggle, P. J., Menezes, R. and Su, T. (2010) Geostatistical inference under preferential sampling. *J. R. Stat. Soc. Ser. C Appl. Stat.* **59:**191–232.

Dunn, D. C., Boustany, A. M. and Halpin, P. N. (2011) Spatio-temporal management of fisheries to reduce by-catch and increase fishing selectivity. *Fish Fish.* **12:**110−119.

Eriksen, E., Ingvaldsen, R. B., Stiansen, J. E. and Johansen, G. E. (2012) Thermal habitat for 0-group fishes in the Barents Sea; how climate variability impacts their density, length and geographical distribution. *ICES J. Mar. Sci.* **69:**870–879.

Felipe, C. C., Debra, J. M., Fa´bio, H. V. H., Humberto, G. H., Bruno, L. M. and George, H. B. (2011) Spatial predictions of blue shark (*Prionace glauca*) catch rate and catch probability of juveniles in the Southwest Atlantic. *ICES J. Mar. Sci.* **68:**890–900.

Fournier, D. A., Skaug, H. J., Ancheta, J., Ianelli, J., Magnusson, A., Maunder, M. N., Nielsen, A. and Sibert, J. (2012) AD Model Builder: using automatic differentiation for statistical inference of highly parameterized complex nonlinear models. *Optimization Methods and Software* **27:**233–249.

Greven, S. and Kneib, T. (2010) On the behaviour of marginal and conditional AIC in linear mixed models. *Biometrics* **97:**773–789.

Hasunuma, K. (1978) Formation of the intermediate salinity minimum in the northwestern Pacific Ocean. *Bull. Ocean Res. Inst.* Univ. Tokyo, 9.

Hiraoka, Y., Kanaiwa, M., Ohshimo, S., Takahashi, N., Kai, M. and Yokawa, K. (2016) Relative abundance trend of the blue shark *Prionace glauca* based on Japanese distant-water and offshore longliner activity in the North Pacific. *Fish. Sci.* **82:**687−699. doi:10.1007/s12562-016-1007-7

Hoeting, J. A., Davis, R. A., Merton, A. A. and Thompson, A. E. (2006) Model selection for geostatistical models. *Ecol. Appl.* **16:**87−98.

Howell, P. and Auster, P. J. (2012) Phase shift in an estuarine finfish community associated with warming temperatures. *Mar. Coast. Fish.* **4:**481–495.

Inoue, R., Yoshida, J., Hiroe, Y., Komatsu, K., Kawasaki, K. and Yasuda, I. (2003) Modification of North Pacific Intermediate Water around Mixed Water Region. *J. Oceanogr*. **59:**211–224.

Ishimura, G. and Bailey, M. (2013) The market value of freshness: observations from the swordfish and blue shark longline fishery. *Fish. Sci*. **79:**547 −533.

Ito, S., Okunishi, T., Kishi, M. J. and Wang, M. (2013) Modelling ecological responses of Pacific saury (*Cololabis saira*) to future climate change and its uncertainty. *ICES J. Mar. Sci*. **70:**980–990.

Jansen, T., Kristensen, K., Kainge, P., Durholtz, D., Strømme, T., Thygesen, U. H., Wilhelm, M. R., Kathena, J., Fairweather, T. P., Paulus, S., Degel, H., Lipinski, M. R. and Beyer, J. E. (2016) Migration, distribution and population (stock) structure of shallow-water hake (*Merluccius capensis*) in the Benguela Current Large Marine Ecosystem inferred using a geostatistical population model. *Fish. Res.* **179:**156–167. doi:10.1016/j.fishres.2016.02.026.

Kai, M., Shiozaki, K., Ohshimo, S. and Yokawa, K. (2015) Growth and spatiotemporal distribution of juvenile shortfin mako, *Isurus oxyrinchus*, in the western and central North Pacific. *Mar. Freshwater Res.* **66:**1176 −1190.

Kai, M., Thorson, J. T., Piner, K. R. and Maunder, M. N. (2017) Spatio-temporal variation in size-structured populations using fishery data: an application to shortfin mako (*Isurus oxyrinchus*) in the Pacific Ocean. *Can. J. Fish Aquat. Sci.* doi:10.1139/cjfas-2016-0327

Kawai, H. (1972) Hydrography of the Kuroshio Extension. In: Kuroshio Physical Aspects of the Japan Current. H. Stommel, and K. Yoshida (ed.) University of Washington Press, pp. 235–352.

Kishi, M. J., Nakajima, K., Fujii, M. and Hashioka, T. (2009) Environmental factors which affect growth of Japanese common squid, *Todarodes pacificus*, analyzed by a bioenergetics model coupled with a lower trophic ecosystem model. *J. Mar. Syst.* **78:**278–287.

Kishi, M. J., Kaeriyama, M., Ueno, H. and Kamezawa, Y. (2010) The effect of climate change on the growth of Japanese chum salmon (*Oncorhynchus keta*) using a bioenergetics model coupled with a three-dimensional lower trophic ecosystem model (NEMURO). *Deep Sea Res. II.* **57:**1257–1265.

Kristensen, K., Thygesen, U. H., Andersen, K. H. and Beyer, J. E. (2014) Estimating spatio-temporal dynamics of size-structured populations. *Can. J. Fish Aquat. Sci.* **71:**326–336.

Kristensen, K., Nielsen, A., Berg, C. W., Skaug, H. and Bell, B. (2015) TMB: Automatic Differentiation and Laplace Approximation. arXiv preprint arXiv:1509.00660.

Lam, V. W. Y., Cheung, W. W. L., Close, C. and Pauly, D. (2008) Modelling seasonal distribution of pelagic marine fishes and squids. In: Modelling Present and Climate-shifted Distribution of Marine Fishes and Invertebrates. W. W. L. Cheung, V. W. Y. Lam and D. Pauly (ed.) Fisheries Centre Research Reports 16, pp. 51–62.

Lindén, A. and Māntyniemi, A. (2011) Using the negative binomial distribution to model overdispersion in ecological count data. *Ecology* **92:**1414 −1421.

Lindgren, F., Rue, H. and Lindström, J. (2011) An explicit link between Gaussian fields and Gaussian Markov random fields: The SPDE approach. *J. R. Stat. Soc. Ser. B Stat. Methodol.* **73:**423–498.

Maunder, M. N., Sibert, J.R., Fonteneau, A., Hampton, J., Kleiber, P. and Harley, S.J. (2006) Interpreting catch per unit effort data to assess the status of individual stocks and communities. *ICES J. Mar. Sci.* **63:**1373–1385.

McCullagh, P. and Nelder, J. (1989) Generalized Linear Models, Second Edition. Boca. Raton: Chapman and Hall/CRC.

Mitchell, J. D., Collins, K. J., Miller, P. I. and Suberg, L. A. (2014) Quantifying the impact of environmental variables upon catch per unit effort of the blue shark *Prionace glauca* in the western English Channel. *J. Fish. Biol.* **85:**657–670.

Mucientes, G., Queiroz, N., Sousa, L., Tarroso, P. and Sims, D. W. (2009) Sexual segregation of pelagic sharks and the potential threat from fisheries. *Biol. Lett.* **5:**156–159.

Musyl, M. K., Brill, R. W., Curran, D. S., Fragoso, N. M., McNaughton, L. M., Nielsen, A., Kikkawa, B. S. and Moyes, C. D. (2011) Postrelease survival, vertical and horizontal movements, and thermal habitats of five species of pelagic sharks in the central Pacific Ocean. *Fish. Bull.* **109:**341–368.

Nakano, H. (1994) Age, reproduction and migration of blue shark in the North Pacific Ocean. *Bull. Nat. Res. Inst. Far Seas Fish.* **31:**141−256.

Nakano, H and Nagasawa, K. (1996) Distribution of pelagic elasmobranchs caught by salmon research gillnets in the North Pacific. *Fish. Sci*. **62:**860–865.

Nakano, H., Okazaki, M. and Okamoto, H. (1997) Analysis of catch depth by species for tuna longline fishery based on catch by branch lines. *Bull. Nat. Res. Inst. Far Seas Fish*. **34:**43–62.

Nakano, H. and Seki, M. P. (2003) Synopsis of biological data on blue shark, Prionace glauca Linnaeus. *Bull. Fish Res. Agen*. **6:**18–55.

Nielsen, J. R., Kristensen, K., Lewy, P. and Bastardie, F. (2014). A Statistical Model for Estimation of Fish Density Including Correlation in Size, Space, Time and between Species from Research Survey Data. *PLoS ONE* **9**(6)**:** e99151.

Nishida, T. and Chen, D. G. (2004) Incorporating spatial autocorrelation into the general linear model with an application to the yel-lowfin tuna (*Thunnus albacares*) longline CPUE data. *Fish. Res*. **70:**265–274.

Ohshimo, S., Fujinami, Y., Shiozaki, K., Mikihiko, K., Semba, Y., Katsumata, N., Ochi, D., Matsunaga, H., Minami, H., Kiyota, M. and Yokawa, K. (2016) Distribution, body length, and abundance of blue shark and shortfin mako offshore of northeastern Japan, as determined from observed pelagic longline data, 2000-2014. *Fish Oceanogr*. **25:**259–276.doi:10.1111/fog.12149

Pearcy, W. G. (1991) Biology of the transition region. *NOAA Tech. Rep. NMFS* **105:**39–56.

Perry, A. L., Low, P. J., Ellis, J. R. and Reynolds, J. D. 2005. Climate change and distribution shifts in marine fishes. *Science* **308:**1912–1915.

Petitgas, P. (1998) Biomass-dependent dynamics of fish spatial distributions characterized by geostatistical aggregation curves. *ICES J. Mar. Sci.* **55:**443–453. doi.org/10.1006/jmsc.1997.0345

Petitgas, P. (2001) Geostatistics in fisheries survey design and stock assessment: models, variances and applications. *Fish. Fish.* **2:**231–249.

Petitgas, P., Doray, M., Huret, M., Masse, J. and Woillez, M. (2014) Modelling the variability in fish spatial distributions over time with empirical orthogonal functions: anchovy in the Bay of Biscay. *ICES J. Mar. Sci.* **71:**2379–2389. doi.org/10.1093/icesjms/fsu111

Queiroz, N., Humphries, N. E., Noble, L. R., Santos, A. M. and Sims, D. W. (2010) Short-term movements and diving behaviour of satellite-tracked blue sharks *Prionace glauca* in the northeastern Atlantic Ocean. *Mar. Ecol. Prog. Ser*. **406:**265–279.

Queiroz, N., Humphries, N. E., Noble, L. R., Santos, A. M. and Sims, D. W. (2012) Spatial Dynamics and Expanded Vertical Niche of Blue Sharks in Oceanographic Fronts Reveal Habitat Targets for Conservation.

PLoS ONE **7(2):**e32374.

R Development Core Team (2013) R: a language and environment for statistical computing. R Foundation for Statistical Computing, Vienna, Austria. ISBN 3-900051-07-0. Available at http://www.R-project.org.

Reid, J. L. (1965) Intermediate waters of the Pacific Ocean. Johns Hopkins Oceanographic Studies, 2, Johns Hopkins Press.

Roa-Ureta, R. and E. Niklitschek. (2007) Biomass estimation from surveys with likelihood based geostatistics. *ICES J. Mar. Sci.* **64:**1723–1734.

Roden, G. I. (1991) Subarctic–subtropical transition zone of the North Pacific: large–scale aspects and mesoscale structure. *NOAA Tech. Rep. NMFS* **105:**1–38.

Shelton, A. O., Thorson, J. T., Ward, E. J. and Feist, B. E. (2014) Spatial semiparametric models improve estimates of species abundance and distribution. *Can. J. Fish Aquat. Sci.* **71:**1655 −1666.

Siders, Z. A., Westgate, A. J., Johnston, D. W., Murison, L. D. and Koopman, H. N. (2013) Seasonal variation in the spatial distribution of basking sharks (*Cetorhinus maximus*) in the lower Bay of Fundy, Canada. *PLoS ONE* **8 (12):**e82074.

Stevens, J. D. (2010) Satellite tagging of blue sharks (*Prionace glauca*) and other pelagic sharks off eastern Australia: depth behaviour, temperature experience and movements. *Mar. Biol.* **157:**575–591.

Stoner, A. W. (2004) Effects of environmental variables on fish feeding ecology: implications for the performance of baited fishing gear and stock assessment. *J. Fish. Bio.* **65:**1445–1471.

Stroup, W.W. (2012) Generalized Linear Mixed Models: Modern Concepts, Methods and applications, Chapman & Hall/CRC.

Su, N. J., Sun, C. L., Punt, A. E., Yeh, S. Z. and Gerard, D. (2011) Modelling the impacts of environmental variation on the distribution of blue marlin, *Makaira nigricans*, in the Pacific Ocean. *ICES J. Mar. Sci.* **68:**1072 −1080.

Suzuki, Z., Warashina, Y. and Kishida, M. (1977) The comparison of catches by regular and deep tuna longline gears in the western and central equatorial Pacific. *Bull. Nat. Res. Inst. Far Seas Fish.* **15:**51−89.

Thorson, J. T., Ianelli, J. N., Munch, S. B., Ono, K. and Spencer, P. D. (2015a). Spatial delay-difference models for estimating spatiotemporal variation in juvenile production and population abundance. *Can. J. Fish. Aquat. Sci.* **72:**1897–1915. doi:10.1139/cjfas-2014-0543.

Thorson, J. T., Shelton, A. O., Ward, E. J. and Skaug, H. (2015b) Geostatistical delta-generalized linear mixed models improve precision for estimated abundance indices for West Coast groundfishes. *ICES J. Mar. Sci.*

72:1297 −1310.

Thorson, J. T., Skaug, H., Kristensen, K., Shelton, A. O., Ward, E. J., Harms, J. and Benante, J. (2015c) The importance of spatial models for estimating the strength of density dependence. *Ecology* **96:**1202–1212.

Thorson, J.T., Fonner, R., Haltuch, M., Ono, K. and Winker, H. 2016. Accounting for spatio-temporal variation and fisher targeting when estimating abundance from multispecies fishery data. *Can. J. Fish. Aquat. Sci*. doi:10.1139/cjfas-2015-0598.

Walsh, W. A. and Kleiber, P. (2001) Generalised additive model and regression tree analyses of blue shark (*Prionace glauca*) catch rates in the Hawaii-based commercial longline fishery. *Fish. Res.* **53:**115–131. doi: 10.1016/S0165-7836(00)00306-4

Walter, J. F., Hoenig, J. M. and Christman, M. C. (2014) Reducing bias and filling in spatial gaps in fishery-dependent catch-per-unit-effort data by geostatistical prediction, I. Methodology and simulation. *N. Am. J. Fish Manage.* **34:**1095–1107.

Ward, E. J., Jannot, J. E., Lee, Y. W., Ono, K., Shelton, A. O. and Thorson, J. T. (2015) Using spatiotemporal species distribution models to identify temporally evolving hotspots of species co-occurrence. *Ecol. Appl.* **25:**2198–2209.

Ward, P. and Myers, R. A. (2005) Shifts in open-ocean fish communities coinciding with the commencement of commercial fishing. *Ecology* **86:**835–847.

Wood, S. N. (2006) Generalized Additive Models, An Introduction with R. Boca. Raton: Chapman and Hall/CRC.

Yasuda, I., Okuda, K. and Shimizu, Y. (1996) Distribution and modification of the North Pacific Intermediate Water in the Kuroshio-Oyashio Interfrontal zone. *J. Phys. Oceanogr.* **26:**448–465.

Yasuda, I., Tozuka, T., Noto, M. and Kouketsu, S. (2000) Heat balance and regime shifts of the mixed layer in the Kuroshio Extension. *Prog. Oceanogr*. **47:**257–278.

Yasuda, I. (2003) Hydrographic structure and variability in the Kuroshio-Oyashio Transition Area. *J. Oceanogr.* **59:**389–402.

Yasuda, T., Yukami, R. and Ohshimo, S. (2014) Fishing ground hotspots reveal long-term variation in chub mackerel *Scomber japonicas* habit in the East China Sea. *Mar. Ecol. Prog. Ser.* **501:**239 −250.

Yoon, S., Watanabe, E., Ueno, H. and Kishi, M. J. (2015) Potential habitat for chum salmon (*Oncorhynchus keta*) in the Western Arctic based on a bioenergetics model coupled with a three-dimensional lower trophic ecosystem model. Progress in Oceanography. *Prog. Oceanogr.* **131:**146–158.

Yoshinari, H., Yasuda, I., Ito, S., Firing, E., Matsuo, Y., Kato, O. and Shimizu, Y. (2001) Meridional transport of the North Pacific Intermediate Water in the Kuroshio-Oyashio interfrontal zone. *Gephys. Res. Lett.* **28:**3445–3448.

Young, J. W., Lamb, T. D., Bradford, R. W., Clementson, L. and Kloser, R. (2001) Yellowfin tuna (*Thunnus albacares*) aggregations along the shelf break off south-eastern Australia: links between inshore and offshore processes. *Mar. Freshwater Res.* **52:**463–474.

Tables

Table 1. Summary of the model selection information for two species from twelve analyses, including the catch rate predictor as random effect and sea surface temperature (SST), the number of parameters, the deviance, the reduction in AIC (ΔAIC) from the best-fitting model, maximum gradient, marginal standard deviation (SD) of spatial variation and spatio-temporal variations. M-7 for shortfin mako, M-7 and M-10 for blue shark were not converged and not shown in the values (grey rows).

Species	Model	Catch rate predictors of random effect (RE)	Number of parameters	Deviance	ΔAIC	Maximum gradient	Marginal SD of spatial variation	Marginal SD of spatio-temporal (year-quarter) variation	Marginal SD of spatio-temporal (quarter) variation
Shortfin mako									
	M-1	Null	22	16706	831	< 0.0001			
	M-2	Station	24	16374	503	< 0.0001	0.706		
	M-3	Year-quarter and station	25	15937	69	< 0.0001		0.925	
	M-4	Station + Quarter and station	26	15987	120	< 0.0001	0.001		0.945
	M-5	Station + Year-quarter and station	26	15921	54	< 0.0001	0.320	0.844	
	M-6	Station + Quarter and station + Year-quarter and station	28	15875	13	< 0.0001	0.0003	0.655	0.547
	M-7	SST	24			0.578			
	M-8	Station + SST	26	16273	407	< 0.0001	1.251		
	M-9	Year-quarter and station+ SST	27	15913	49	< 0.0001		0.888	
	M-10	Station + Quarter and station + SST	28	15974	112	< 0.0001	0.001		0.956
	M-11	Station + Year-quarter and station + SST	28	15898	35	< 0.0001	0.314	0.811	
	M-12	Station + Quarter and station + Year-quarter and station + SST	30	15858	0	< 0.0001	0.00004	0.646	0.512
Blue shark									
	M-1	Null	22	31195	2383	< 0.0001			
	M-2	Station	24	29437	629	< 0.0001	1.024		
	M-3	Year-quarter and station	25	28910	104	< 0.0001		1.100	
	M-4	Station + Quarter and station	26	29105	302	< 0.0001	0.433		0.972
	M-5	Station + Year-quarter and station	26	28844	41	< 0.0001	0.567	0.764	
	M-6	Station + Quarter and station + Year-quarter and station	28	28812	13	< 0.0001	0.237	0.627	0.616
	M-7	SST	24			0.009			
	M-8	Station + SST	26	29425	621	< 0.0001	0.821		
	M-9	Year-quarter and station+ SST	27	28889	87	< 0.0001		0.966	
	M-10	Station + Quarter and station + SST	28			0.012			
	M-11	Station + Year-quarter and station + SST	28	28824	24	< 0.0001	0.471	0.722	
	M-12	Station + Quarter and station + Year-quarter and station + SST	30	28796	0	< 0.0001	0.200	0.608	0.527

Table 2. Quantiles of sea surface temperature (°C, where 50% is the median temperature, 0% is the lowest temperature, and 100% is the highest temperature) of the preferred habitat of shortfin mako and blue sharks (defined as locations where the predicted catch rate relative value to mean value of each shark was more than 1.0).

Sea surface temperature (°C)

	0%	25%	50%	75%	100%
Shortfin Mako					
Quarter 1	9.9	16.3	17.8	19.0	21.8
Quarter 2	10.0	16.8	18.6	19.7	21.5
Quarter 3	14.9	20.3	22.7	24.9	27.0
Quarter 4	10.4	18.1	20.5	22.5	23.8
All quarters	9.9	17.5	19.2	21.5	27.0
Blue shark					
Quarter 1	6.3	11.5	13.8	15.8	19.1
Quarter 2	6.5	12.8	14.7	16.9	20.4
Quarter 3	14.9	19.8	21.8	23.6	26.5
Quarter 4	9.4	16.1	18.1	20.1	23.2
All quarters	6.3	13.9	16.7	19.8	26.5

Figure Legends

Fig. 1. Map of schematic Kuroshio (warm water) and Oyashio (cold water) currents, Kuroshio-Oyashio Transition Zone (TZ), Mixed water region between subarctic current and Kuroshio extension, and Emperor Seamount Chain in the western and central North Pacific.

Fig. 2. Seasonal changes of the spatial distributions of predicted catch rate relative its average for shortfin mako and blue shark (left and mid figures). Contours denote the isothermal lines of sea surface temperature (°C). We also plot the number of hooks (logscale), representing the distribution of available data (right figures).

Fig. 3. Time (year-season) specific changes of the spatial distributions of predicted catch rate relative its average (logscale) for the data of shortfin mako. Contours denote the isothermal lines of sea surface temperature (°C) and blue, green, orange, brown, and red lines indicate 5°C, 10°C, 15°C, 20°C, and 25°C, respectively. The figures were plotted using the values derived from Eq. (1).

Fig. 4. Time (year-season) specific changes of the spatial distributions of predicted catch rate relative its average for blue shark. Contours denote the isothermal lines of sea surface temperature (°C) and blue, green, orange, brown, and red lines indicate 5 °C, 10 °C, 15 °C, 20 °C, and 25 °C, respectively. The figures were plotted using the values derived from Eq.(1).

Fig. 5. Seasonal changes of predicted catch rate (relative value to mean value, such that the dashed line at 1.0 represents the mean catch rate) against mean SST (sea surface temperature) (°C), for shortfin mako and blue shark with marginal density plots showing the distribution of temperature in preferred habitats (defined as locations where the catch rate was greater than the mean). A point in the bottom row indicates each station in each quarter (where quarters are color coded).

687

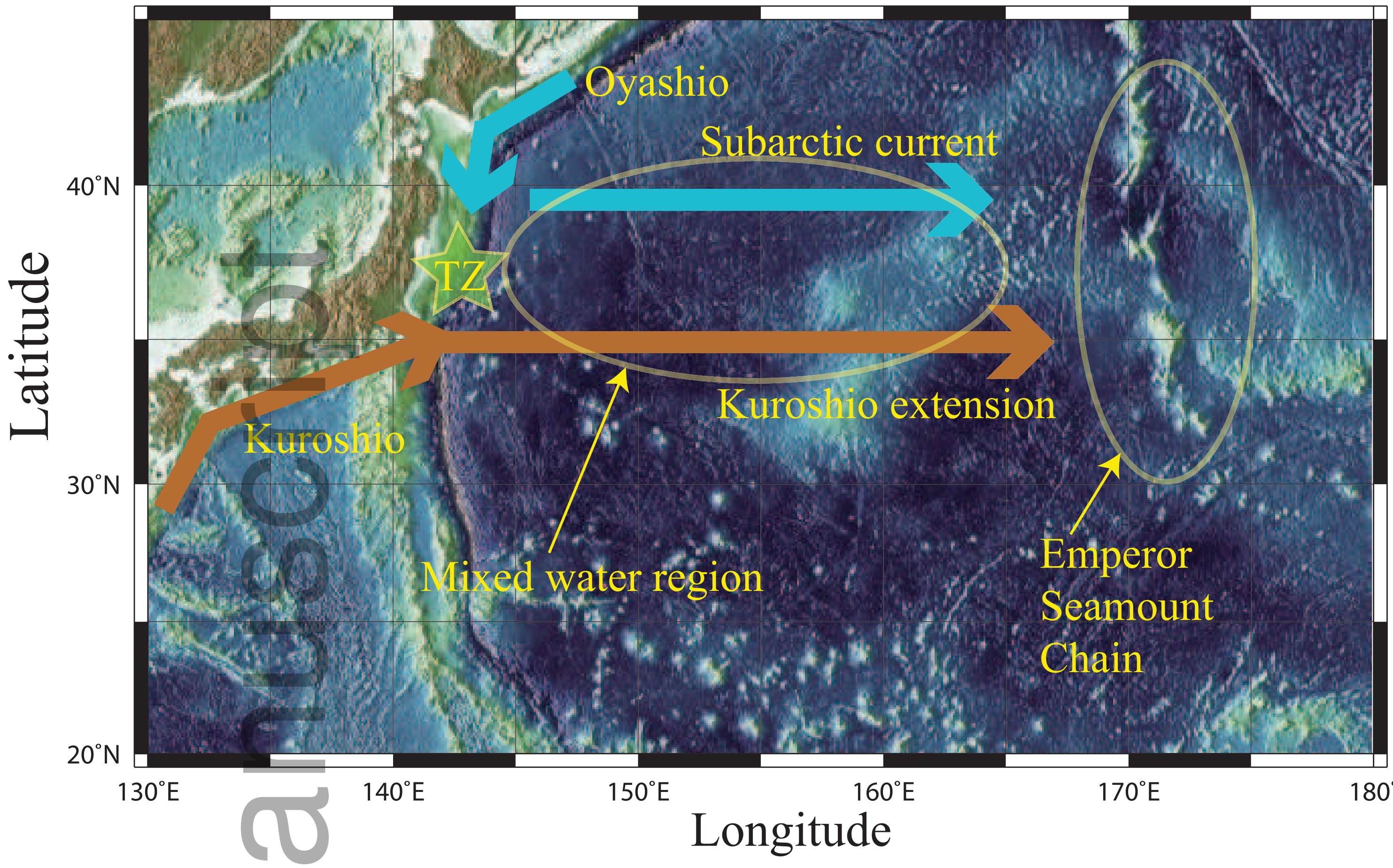

fog_12217_f1.eps

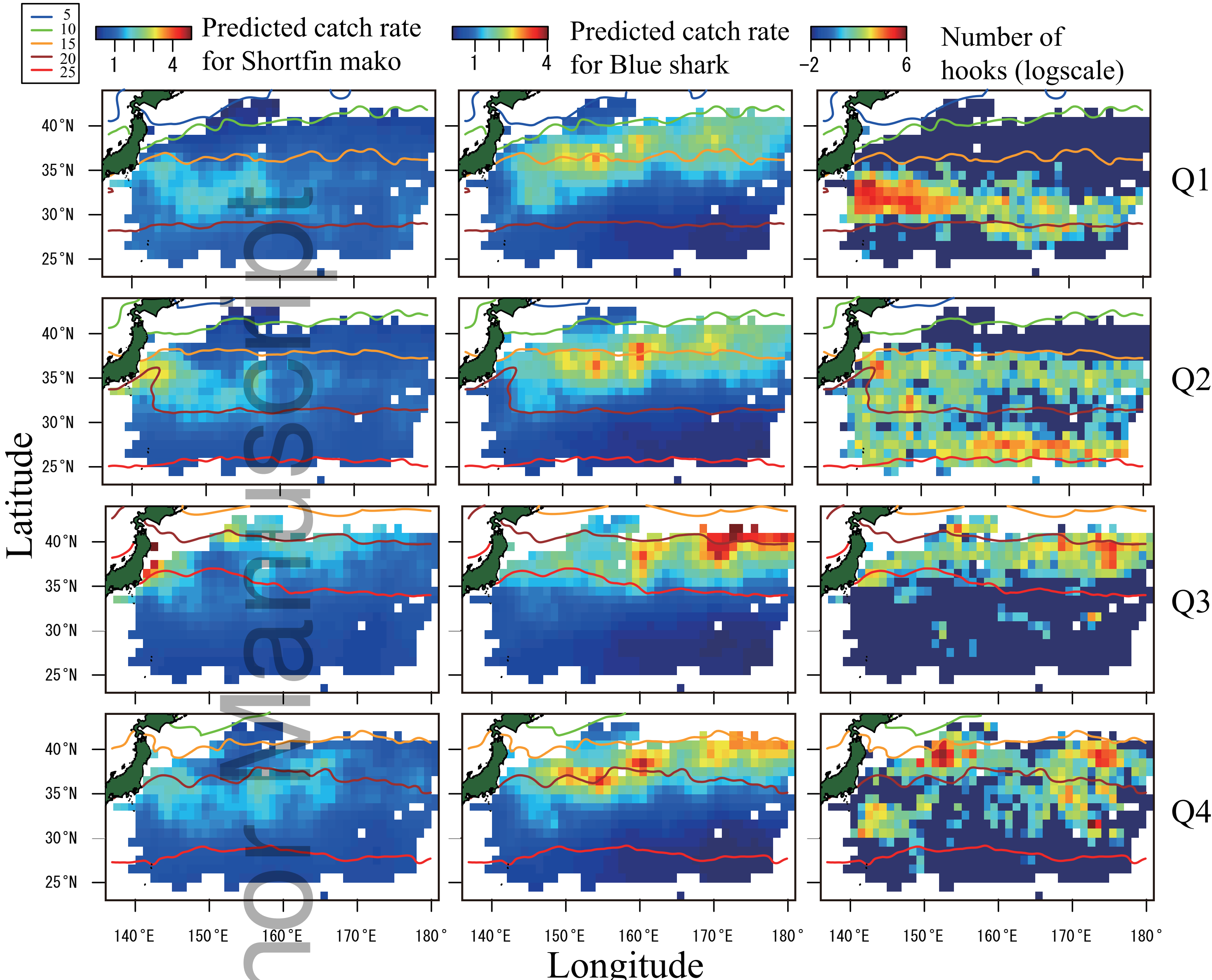

fog_12217_f2.eps

fog_12217_f3.eps

fog_12217_f4.eps

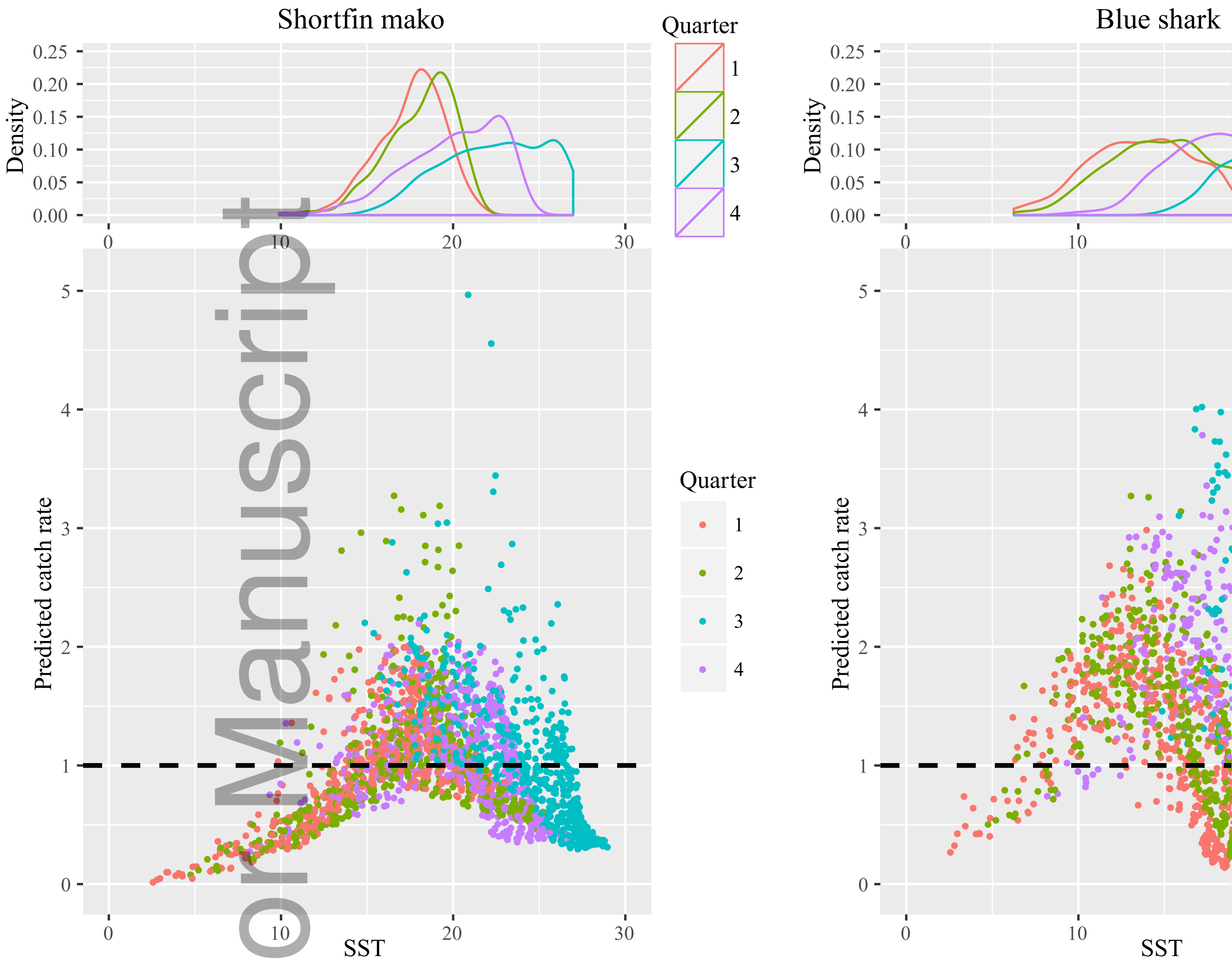

fog_12217_f5.eps